RSC Advances

PAPER

View Article Online
View Journal | View Issue

Cite this: *RSC Adv.*, 2022, **12**, 21982

Preparation, characterization and *in vitro* study of bellidifolin nano-micelles

Fan Gao, †[a] Ziyue Chen,†[b] Li Zhou,[a] Xuefeng Xiao,[b] Lin Wang,[c] Xingchao Liu,[a] Chenggang Wang*[c] and Qiuhong Guo*[a]

Bellidifolin (BEL), a xanthone compound, has significant therapeutic effectiveness in cardiac diseases such as arrhythmias. However, BEL is limited in clinical applications by its hydrophobicity. In this work, we used BEL as the active pharmaceutical ingredient (API), and polyethylene glycol 15-hydroxy stearate (Kolliphor HS15) as the carrier to prepare BEL nano-micelles by a solvent-volatilization method. According to an analysis by differential scanning calorimetry (DSC), BEL was successfully encapsulated in HS15 as BEL nano-micelles with a 90% encapsulation rate, and particle size was 12.60 ± 0.074 nm in the shape of a sphere and electric potential was −4.76 ± 4.47 mV with good stability and sustained release characteristics. In addition, compared with free drugs, these nano-micelles can increase cellular uptake capacity, inhibit the proliferation of human cardiac fibroblasts, and down-regulate the expression of Smad-2, α-SMA, Collagen I, and Collagen III proteins in myocardial cells to improve myocardial fibrosis. In conclusion, the BEL nano-micelles can provide a new way for the theoretical basis for the clinical application of anti-cardiac fibrosis.

Received 2nd May 2022
Accepted 9th July 2022

DOI: 10.1039/d2ra02779h

rsc.li/rsc-advances

1 Introduction

Myocardial fibrosis (MF) is a common pathological phenomenon in the late stage of a variety of heart diseases, which is characterized by excessive deposition of extracellular matrix (ECM) protein in the myocardium, which distorts the myocardial structure, resulting in arrhythmias and cardiac dysfunction by impairing cardiac contraction and diastolic functions and dysregulation of excitation-contraction coupling. More seriously, MF may develop into sudden cardiac death and heart failure.[1] Therefore, taking appropriate measures to prevent and treat myocardial fibrosis is expected to delay the development of heart disease, which is of great significance to improve people's health status and quality of life.

Bellidifolin (BEL), is a xanthone compound, which molecular formula is $C_{14}H_{10}O_6$ and whose molecular weight is 274.22 g mol^{-1}. BEL is a yellowish powder that insoluble in water. Fig. 1 shows the chemical formula of BEL. BEL is the main active ingredient of Mongolian medicine Gentianella acuta (Michx.) Hulten.[2,3] It is commonly known as a "Stable heart herb". Residents in Inner Mongolia brew it instead of tea, which can prevent and treat cardiac arrhythmia and other heart diseases with significant effects.[4] Some research groups have found that Gentiana can reverse isoproterenol-induced myocardial fibrosis in rats and improve cardiac function through anti-oxidation, inhibiting the inflammatory signaling pathway of myocardial tissue and down-regulating the expression of Galectin-3, NF-κB-P65, TGF-β1, and CTGF.[5,6] Gentian can also inhibit isoproterenol-induced myocardial fibrosis in rats by down-regulating TGF-β1, inhibiting phosphorylation of TGF-β receptor I/II, and blocking the activation of the TGF-β1/Smads signaling pathway.[6] In this study, the pharmacodynamics of BEL was further studied. In mice, BEL inhibited isoproterenol-induced cardiac structure disorder and collagen deposition. *In vitro*, BEL inhibited the proliferation of myocardial fibroblasts induced by TGF-β1. Both cell and animal studies have proved

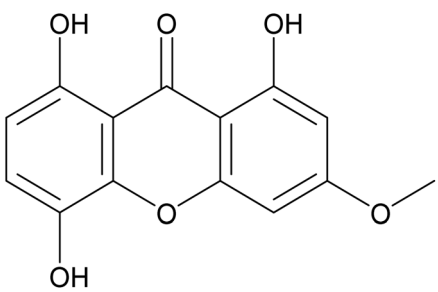

Fig. 1 The chemical formula of BEL.

[a]*Hebei TCM Formula Preparation Technology Innovation Center, Hebei University of Chinese Medicine, Shijiazhuang 050091, People's Republic of China. E-mail: qiuhong70105@163.com*

[b]*School of Chinese Materia Medica, Tianjin University of Traditional Chinese Medicine, Tianjin 301617, People's Republic of China*

[c]*State Key Laboratory of Drug Delivery Technology and Pharmacokinetics, Tianjin Institute of Pharmaceutical Research, Tianjin 300301, People's Republic of China. E-mail: wangcg@tipr.com.cn*

† These authors contributed equally to this work, and Z. Chen is the co-first author for this paper.

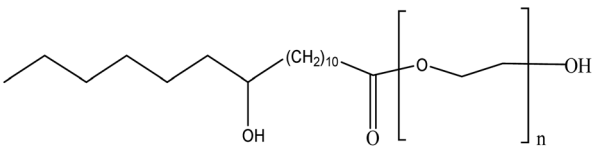

Fig. 2 Kolliphor HS15 chemical structure formula.

that BEL has a potential effect on myocardial fibrosis.[7] However, the insoluble nature of BEL limits its applications in clinical.

Nano-micelles are amphiphilic polymers formed by hydrophilic (such as PEG, PVP) and lipophilic (such as PET, PCPP-SA) parts with nanoscale core–shell structure. Because of their inherent properties, they are particularly well suited for drug delivery systems (DDS). Due to the inherent structural properties of nano-micelles, their advantages include (1) protecting encapsulated drugs against degradation *in vitro*,[8](2) circulating in the blood for a long time and releasing drugs gradually, (3) being suitable for carrying drugs through the intestinal mucus layer and reaching the intestinal epithelial cells and increasing the absorption of drugs in the intestinal tract with the small size of particles.[9] They can also contain toxic or insoluble compounds in the allowable dose range for safe application. Most of these advantages are related to the hydrophilic part, especially the PEG part. Nanostructured systems with low cost, low toxicity, stability in aqueous media, and high hydration degree have important application value in pharmacology.[10] For example, Genexol® PM, a micelle formulation of paclitaxel approved by the FDA, is used for the therapeutic of breast, lung, and ovarian cancers.[11]

Kolliphor®HS15 (Polyoxyl 15 hydroxy stearate, HS15) is novel non-ionic surfactant developed by BASF Aktiengesellschaft. It is a composite material comprising polyglycerol esters of 12-hydroxystearic acid (70%) combined with free polyethylene glycol (30%) and has a monograph in the European, US, and Japanese Pharmacopoeias.[12] Fig. 2 shows the chemical structure formula of Kolliphor HS15. It is widely used to increase drug solubility, enhance absorption and improve drug bio availability.[13,14] In order to improve the stability and solubility of coenzyme Q10, Liu[15] *et al.* established a stable nano-micelle delivery system to carry Coenzyme Q10, using HS15 as the carrier. After reviewing the literature, there are few reports about the preparation that can increase the solubility of BEL. Therefore, we prepared BEL into nano micelle to research the physical properties and compare BEL nano micelle (BEL@HS15) with free drug resistance *in vitro* myocardial fibrosis, in order to lay a foundation for further preclinical studies.

2 Materials and methods

2.1 Materials

Bellidifolin was purchased from Alfa (China). Kolliphor HS15 was purchased from BASF(GER). Human Cardiac Fibroblast Cells (HCF) were provided by the Hebei University of Chinese Medicine (China). Dulbecco's modified Eagle's medium (DMEM), fetal calf serum were purchased from Gibco (USA). Phosphate Buffered Saline (PBS), Hoechst33342, Antifade Mounting Medium was purchased from Biosharp (China). Pyrene was purchased from Macklin (China). Coumarin-6 was purchased from Aladdin (China). TGF-β1 was purchased from Novoprotein (China). Cell Counting Kit-8 (CCK-8) was purchased from HaiGene Technology (China). Smad-2 ELISA Kit, α-SMA ELISA Kit, Collagen I ELISA Kit, Collagen III ELIAS Kit were purchased from Fine Text (China). Acetone, Methanol, and Acetonitrile (HPLC grade) were purchased from Kemiou (China).

2.2 Preparation of BEL@HS15

BEL@HS15 was prepared by the solvent evaporation method. A certain amount of Kolliphor HS15 was dissolved in 10 mL pure water, and 1 mg of BEL was dissolved in 1 mL acetone. The acetone solution was slowly added to the pure water while stirring with magnetic force and heated with magnetic stirring. A 0.45 μm microporous membrane was used to remove the free drugs, and a clear yellow micellar solution was obtained. Through the previous orthogonal experiment, the optimal preparation process conditions were optimized. The concentration of HS15 was 30 mg mL^{-1}, and the concentration of BEL was 0.102 mg mL^{-1}.

2.3 Characterization of BEL@HS15

2.3.1 The encapsulation entrapment rate (EE) of BEL@HS15. The encapsulation entrapment rate (EE) of BEL@HS15 was determined as follows. The prepared BEL@HS15 solution was absorbed, and a certain amount of methanol solution was added for ultrasonic demulsification (300 W, 40 kHz), and then 0.22 μm microporous membrane was used for filtration. The peak area was recorded by High-performance liquid chromatography (HPLC, ShimadzuLC-20AD, Japan), and the mass of the encapsulated drugs in the micelles was calculated. The encapsulation rate (EE%) was calculated according to the following formula (1).

$$\mathrm{EE\%} = \frac{\text{The amount of drug contained in micelles/mg}}{\text{Total drug input/mg}} \times 100\% \quad (1)$$

2.3.2 The particle size and zeta potential of BEL@HS15. The particle size and zeta potential of BEL@HS15 (HS15,30 mg mL^{-1}; BEL, 0.102 mg mL^{-1}) were determined by Laser particle size analyzer (Zetasizer Nano ZS90, France). Take BEL@HS15 solution was placed in the cuvette. The temperature was kept at 25 °C during the measuring process, and all results were the mean of three different samples.

2.3.3 The morphology of BEL@HS15. The morphology of BEL@HS15 (HS15,30 mg mL^{-1}; BEL, 0.102 mg mL^{-1}) morphology was observed under a transmission electron microscope (TEM, JEM-2100F, JEOL, Japan). The appropriate amount of the prepared micelle solution was dropped onto the copper net, placed in a drying box, set the temperature at 37 °C, dried to form a film, and removed for observation.

2.3.4 Determination of critical micelle concentration(CMC) of HS15. The critical micelle concentration of HS15 was determined by using pyrene as fluorescence probe. 300 mg HS15 was dissolved in 10 mL ultra-pure water, heated at 35 °C and stirred with magnetic force for 0.5 h. The solution was diluted to a concentration of 20–200 μg mL^{-1}, and 1 mL pyrene acetone solution was added to each concentration for 24 h at constant temperature, so that the final concentration of pyrene was 4×10^{-7} mol L^{-1}. The excitation wavelength was set at 335 nm. The emission wavelengths were 373 nm and 394 nm. Under these conditions, the fluorescence spectrophotometer was used for detection, and the relationship between the ratio of I_{373}/I_{394} and micellar concentration was recorded.

2.3.5 Differential scanning calorimetry (DSC) analysis. The physical mixture of BEL and HS15, BEL, HS15 and the freeze-dried powder BEL@HS15 (HS15,30 mg mL^{-1}; BEL, 0.102 mg mL^{-1}) were respectively put into the sample crucible and raised from room temperature to 500 °C at the speed of 10 °C min^{-1} in a nitrogen atmosphere. Thermal analysis of each sample was carried out under these conditions by differential scanning calorimetry (DSC, Mettler Toledo DSC3, Swiss).

2.3.6 *In vitro* release. The release of BEL monomer and the micelle *in vitro* was compared by the dialysis method. 1.00 mg BEL was precisely weighed, dissolved BEL with dimethyl sulphoxide, and the micelle solution containing the same quality BEL was placed in dialysis bags (3000–4000), sealed firmly, and placed in a 20 mL pH7.4 PBS release medium. Because the drug is lipid-soluble, 0.5% Tween 80 was added to the PBS to meet the sink condition. *In vitro* release characteristics were tested a 37°C-water bath. 1 mL solution was absorbed at time points 1, 2, 4, 6, 8, 12, 24, 36, 48, 60, and 72 h, respectively, while the fresh buffer was added. The solution was detected by HPLC, and release amounts at different time points were calculated according to the standard curve. The cumulative release rate at different time points was calculated according to the following formula (2).

$$E_r = \frac{V_e \sum_{1}^{n-1} C_i + V_0 C_n}{m_{drug}} \times 100\%^{16} \quad (2)$$

E_r is the cumulative release rate, V_e is the volume absorbed each time (mL), C_i is the drug concentration of the ith sample (μL mL^{-1}), V_0 is the volume of the release medium (mL), C_n is the drug concentration of the Nth sample (μL mL^{-1}), n is the number of samples, where $i = n - 1$ ($n > 0$), m is the total drug mass.

2.4 Cells on myocardial fibrosis *in vitro* experiments

2.4.1 Cell uptake assay. The fluorescence probe of coumarin-6 (Cou-6) was used to replace the drug, and the encapsulated Cou-6@Kolliphor HS15 was prepared according to the method of preparing BEL @Kolliphor HS15, and the cell uptake of Cou-6 and Cou-6@Kolliphor HS15 was compared. The cells were inoculated into 24-well plates covered with slivers, with 1×10^4 cells in each well, and incubated in an incubator for 24 h and adhered to the wall. Drugs were added for 2 h and 4 h, respectively. After that, the nuclei were stained with Hoechst33342 fluorescent staining agent, the slivers were removed and the drug uptake in the cells was observed under a fluorescence microscope (DMI3000B, Leica, Germany).

2.4.2 Morphological observation of BEL@HS15 effect on HCFs. HCFs in the logarithmic growth phase were inoculated into 96-well plates, with about 2×10^3 cells in each well. The Control group, model group, and drug group were set up. After cell adherence for 24 h, the old solution was sucked and discarded, and serum-free DMEM starvation treatment was added for 24 h. In the drug group, BEL@HS15 and 20 ng mL^{-1} TGF-β1 were added and incubated for 24 h, then removed from the incubator, and cell morphology of each group was observed under an inverted microscope (ZEISS, German).

2.4.3 CCK-8 method was used to determine the inhibiting rate of cell proliferation. The cells were inoculated into 96-well plates with about 2×10^3 cells in each well, which were divided into the model group, drug group (containing BEL@HS15 and BEL with drug concentrations of 0.33, 0.495, and 0.66 μg mL^{-1}), control group, and blank group with 5 holes in each group. After 24 h of cell adherence, the old solution was sucked up, and serum-free DMEM starvation treatment was added for 24 h. The model group was induced by adding 20 ng mL^{-1} TGF-β1. The drug group was BEL@HS15 + TGF-β1 20 ng mL^{-1}, BEL + TGF-β1 20 ng mL^{-1}, respectively. The control group only contained cells and medium, and the blank group only contained medium. Discard the old liquid and add fresh culture medium and 10 μL CCK-8, incubated for 1 h, then measured OD value at 450 nm of the microplate (Thermo Fisher Scientific, China) reader.

2.4.4 The expressions of Smad-2, α-SMA, Collagen Iand Collagen III were detected by ELISA. Myocardial fibroblasts in the logarithmic growth phase were inoculated into 6-well plates with about 5×10^5 cells in each well. The experiment was divided into control group, model group, BEL group, and BEL@HS15 group. After cell adherence, the old medium was absorbed and discarded. The control group was added to a fresh medium, the model group was added with TGF-β1 (20 ng mL^{-1}), and the BEL@HS15 group was added with different concentrations of nano-micelles (0.33, 0.495 and 0.66 μg mL^{-1}) + TGF-β1 (20 ng mL^{-1}). BEL group was added with different concentrations of BEL (0.33, 0.495 and 0.66 μg mL^{-1}) + TGF-β1 (20 ng mL^{-1}). Each group was stimulated for 24 h.

HCFs supernatant was collected from each group, and the expression of Collagen I and Collagen III secreted by cells was detected by the ELISA kit. The old cell culture medium of each group was absorbed and discarded, the cells were washed with PBS 3 times, the cell lysate was added, and the cells were detached by operation on ice. After the lysate was completed, the cells were centrifuged at 12000 rpm at 4 °C for 10 min. HCFs supernatant of each group was collected, and the expressions of Smad-2 and α-SMA in the cells were detected by ELISA kit. The experimental procedures are carried out in strict accordance with the instructions.

2.5 Statistical analyses

The statistical analysis software SPSS22.0 for Windows (SPSS Inc., Chicago, IL, USA) was used. The results are recorded as

mean ± standard deviation (SD). Analysis of variance (ANOVA) was employed for multiple group comparisons. $P < 0.05$ was considered statistically significant.

3 Results and discussion

3.1 Characterization of BEL@HS15

3.1.1 The encapsulation entrapment rate (EE) of BEL@HS15. 1.00 mg of BEL was precisely weighed and determined by HPLC. The content of the encapsulated drug in the nano-micelles was calculated to be 0.90 mg, so the encapsulation rate

$$\mathrm{EE}\% = \frac{\text{The amount of drug contained in micelles/mg}}{\text{Total drug input/mg}} \times 100\% = \frac{0.90\ \text{mg}}{1.00\ \text{mg}} \times 100\% = 90\%.$$

3.1.2 The particle size and zeta potential of BEL@HS15. The particle size measurement results of BEL nano micelles (HS15,30 mg mL^{-1}; BEL, 0.102 mg mL^{-1}) are shown in Fig. 3. From the results, the particle size of the nano micelle is 12.60 nm and the PDI is 0.136.

BEL@HS15 potential distribution as shown in Fig. 4, under the optimum preparation process of preparation of BEL@KolliphorHS15 negatively charged surface, zeta potential for −4.76 MV.

3.1.3 Morphological characterization of BEL@HS15. The results in Fig. 5 show that the nano micelles (HS15,30 mg mL^{-1}; BEL, 0.102 mg mL^{-1}) under TEM were spherical with small particle sizes.

3.1.4 Determination of critical micelle concentration(CMC) of HS15. Results as shown in the Fig. 6. The curve of I_{373}/I_{394} changing with the concentration of HS15 is in line with the rule of Boltzamann curve. Boltzamann curve is adopted for fitting, and the curve equation is as follows:[17]

$$y = A_2 + \frac{A_1 - A_2}{1 + \exp[(x - x_0)\Delta x]} \quad (3)$$

A_1 is I_{373}/I_{394} at low surfactant concentration; A_2 is I_{373}/I_{394} at high surfactant concentration; x is HS15 concentration; x_0 is the CMC of HS15; Δx is the slope of the curve drawn at the midpoint x_0 of the mutation, which intersects with the two straight lines

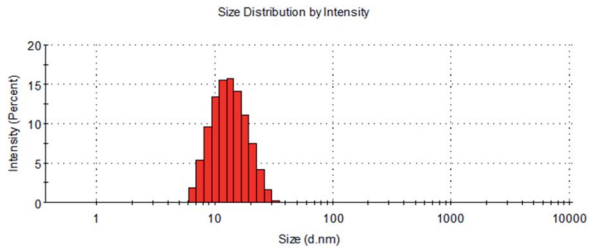

Fig. 3 Particle size distribution of BEI@HS15.

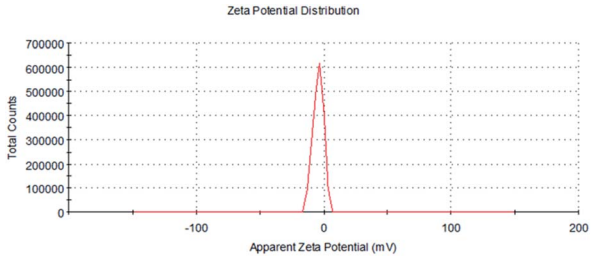

Fig. 4 The zeta distribution of BEI@HS15. HS15, 30 mg mL^{-1}; BEL, 0.102 mg mL^{-1}.

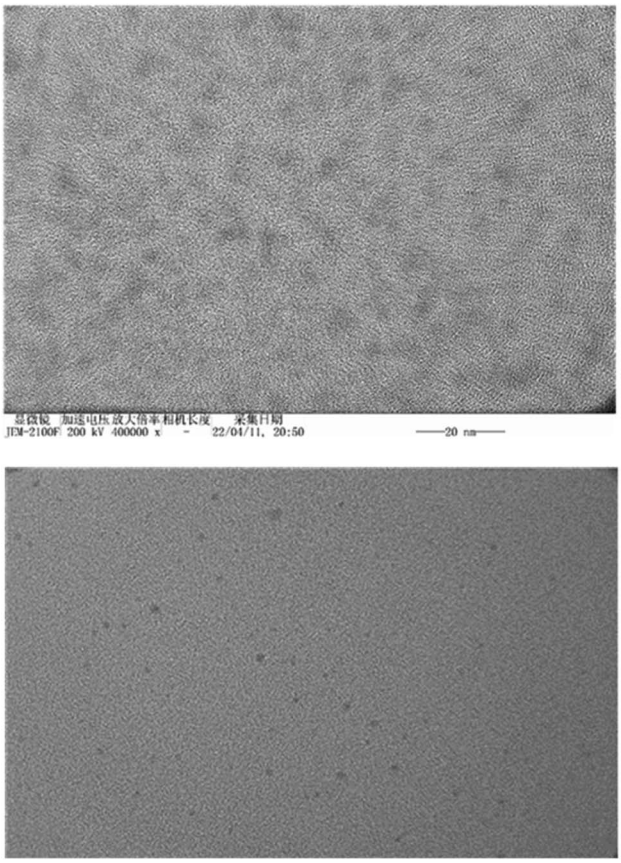

Fig. 5 BEL@HS15 Transmission electron microscope image. HS15, 30 mg mL^{-1}; BEL, 0.102 mg mL^{-1}.

A_1 and A_2 parallel to the X-axis. The value of 1/4 of the horizontal distance between the two intersection points is a parameter describing the degree of mutation of the Boltzamann curve.

X_0 is the CMC of HS15, and the equation obtained by fitting is $y = 1.21 + \frac{1.04 - 1.21}{1 + \exp[(x - 99.74) \times 22.57]}$, $R^2 = 0.9731$, so the CMC of HS15 is 99.74 μg mL^{-1}.

3.1.5 Differential scanning calorimetry (DSC) investigates the interaction between drug and carrier. Fig. 7 shows differential scanning calorimetry of four samples. BEL has endothermic peaks at 81.74 °C, 234.58 °C, and 270.90 °C, respectively. BEL's endothermic peak at 271 °C appears in the physical mixture of BEL and HS15, and BEL's endothermic peak

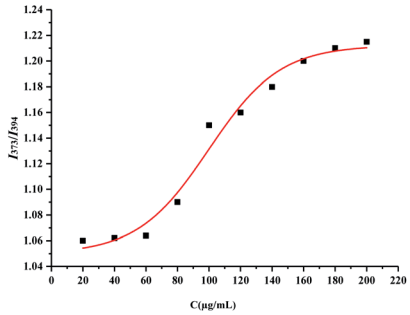

Fig. 6 Curve of I_{373}/I_{394} with HS15 concentration.

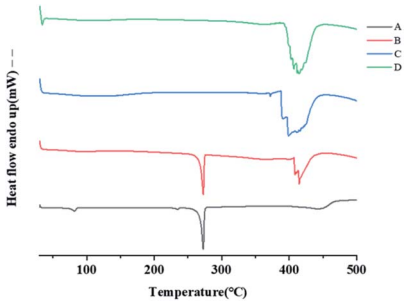

Fig. 7 Differential scanning calorigram. A is BEL; B is physical mixture of BEL and HS15; C is nano-micelles; D is HS15. (HS15, 30 mg mL^{-1}; BEL, 0.102 mg mL^{-1}).

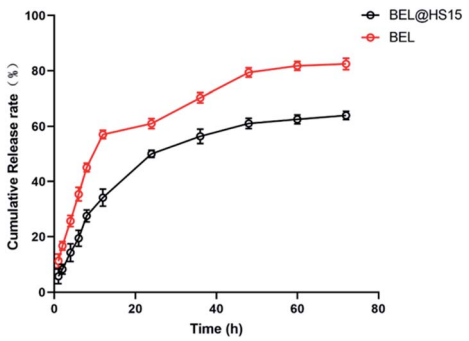

Fig. 8 BEL and BEL@HS15 *in vitro* release curves.

disappears in the BEL nano-micellar, like that of HS15. It indicates that BEL is encapsulated in nano micelles.

3.1.6 *In vitro* release test. As shown in Fig. 8, the overall release of drugs in micellar solution is slow. When the *in vitro* cumulative release rate of BEL@HS15 is 50%, the release time is about 24 h; when the *in vitro* cumulative release rate of drug monomer is 50%, the release time is about 8 h. Compared with drug monomers, the release rate of nano micelles is slow and can achieve the effect of sustained release. Therefore, it can be explained that BEL@HS15 has the characteristics of slow drug release. The measured cumulative release data were curve fitted by Origin2017 software. *In vitro* release models included zero-order release models, first-order release models, Higuchi equation, Weibull distribution model, *etc.* As can be seen from Table 1, BEL@HS15 conforms to the first-order release model with an R^2 value of 0.998. BEL conforms to the Weibull distribution model and the R^2 value is 0.980.

3.2 Cells on myocardial fibrosis *in vitro* experiments

3.2.1 Cell uptake assay. Results as shown in Fig. 9. The fluorescence intensity of nano-micelles absorbed by HCFs cells was higher than that of free drugs after 2 h and 4 h of drug

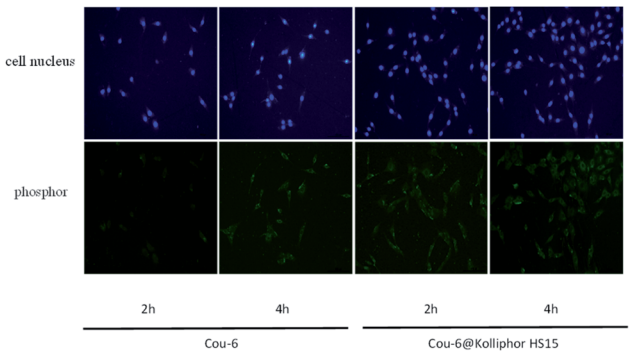

Fig. 9 Cellular uptake of Cou-6 and Cou-6@Kolliphor HS15 (20×).

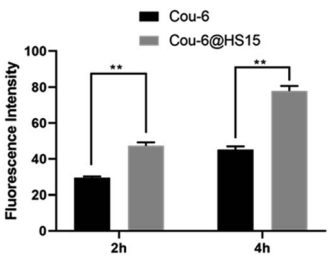

Fig. 10 Cou-6 and Cou-6@HS15 fluorescence intensity. Compared with Cou-6, $^{**}P < 0.01$.

Table 1 Drug release model and correlation coefficient

Emission model	BEL@HS15	R^2 adjusted	BEL	R^2 adjusted
Zero-order release	$E_r = 16.168 + 0.826t$	0.826	$E_r = 28.358 + 0.932t$	0.786
First-order release	$E_r = 63.787(1 - e^{-0.065t})$	0.998	$E_r = 78.03(1 - e^{-0.100t})$	0.967
Higuchi equation	$E_r = 8.408t^{1/2} + 0.585$	0.948	$E_r = 9.559t^{1/2} + 10.450$	0.919
Weibull model	$E_r = 100\left(1 - e^{\frac{-(t-0.785)^{0.576}}{10.122}}\right)$	0.952	$E_r = 100\left(1 - e^{\frac{-(t-0.672)^{0.542}}{5.405}}\right)$	0.980

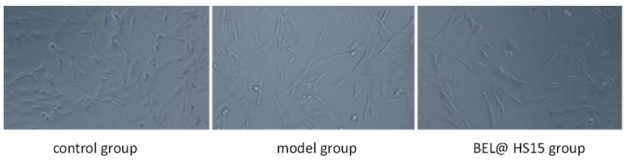

Fig. 11 Morphological observation of TGF-β 1-induced HCFs by BEL@HS15 (200×).

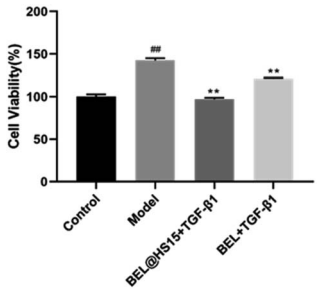

Fig. 12 Effect of BEL and BEL@HS15 on HCFs cell activity. Compared with control group, $^{\#}P < 0.05$, $^{\#\#}P < 0.01$; Compared with model group, $^{*}P < 0.05$, $^{**}P < 0.01$.

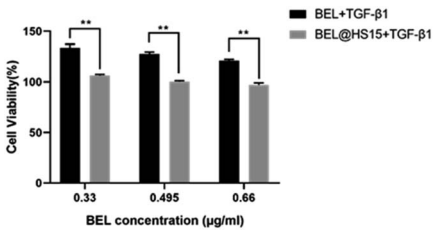

Fig. 13 Effect of BEL and BEL@HS15 on HCFs cell activity at the same concentration. Compared with BEL + TGF-β1, $^{**}P < 0.01$.

stimulation, and the longer the stimulation, the stronger the fluorescence intensity. Using Image-pro Plus software to analyze the fluorescence intensity of the cells in the cell, the fluorescence intensity of the cells was calculated, results as shown in Fig. 10, and the results of the fluorescence intensity of the cells were significantly higher than that of the free drug ($P < 0.01$), and time dependence. The results further demonstrate that the nano-micelles can increase the permeability and liquidity of the membrane, promote the transmembrane transfer of the drug and increase the amount of cell intake of the drug.

3.2.2 Morphological observation of BEL@HS15 effect on HCFs. The cell morphology of each group was observed under an inverted microscope, and the results were shown in Fig. 11. According to the figure, HCFs in the control group were polyangular and full, but after induction by TGF-β1, the cells became elongated, narrow, and fusiform, and the cell morphology improved after drug intervention.

3.2.3 CCK-8 method was used to determine the inhibiting rate of cell proliferation. The results of the effects of BEL and BEL@HS15 on HCFs activity and the results of the effects of BEL and BEL@HS15 on HCFs activity at the same drug concentration are shown in Fig. 12 and 13. Fig. 12 shows that compared with the control group, cell proliferation ability in the model group was significantly up-regulated ($P < 0.01$), compared with the drug group, both BEL@HS15 group and BEL group could significantly inhibit cell proliferation ($P < 0.01$), but it can be seen from Fig. 13 that BEL@HS15 group inhibited cell proliferation more significantly than BEL group ($P < 0.01$), and in a concentration dependent manner, suggesting that BEL@HS15 can effectively inhibit TGF-β1 induced cell proliferation, and further confirming that nano-micelles can increase the permeability of cell membrane, increase drug uptake, and thus improve drug efficacy.

3.2.4 The expressions of Smad-2, α-SMA, Collagen I, and Collagen III were detected by ELISA. The results were shown in Table 2. Compared with the control group, Smad-2, α-SMA, Collagen I, and Collagen III expressions were up-regulated in the model group with significant differences, indicating that myocardial fibroblasts had transformed into myofibroblasts. Compared with the model group, The expression levels of Smad-2, α-SMA, Collagen I, and Collagen III were decreased in the BEL monocyte group, while the expression levels of various indexes were significantly decreased in the BEL@HS15 group, suggesting that BEL@HS15 could significantly inhibit myocardial fibrosis.

Table 2 Comparison of expression of related cytokines in myocardial fibroblasts in each group (ng mL^{-1}, $\bar{x} \pm s$, $n = 3$)[a]

Groups	Smad-2	α-SMA	Collagen I	Collagen III
Control group	2.504 ± 0.06	113.53 ± 1.58	1.02 ± 0.03	2.69 ± 0.14
Model group	3.60 ± 0.04$^{\#\#}$	231.15 ± 18.20$^{\#\#}$	1.60 ± 0.06$^{\#\#}$	8.57 ± 0.59$^{\#\#}$
A_1	3.43 ± 0.08*‡	190.44 ± 5.20**‡	1.51 ± 0.02‡	6.73 ± 0.29**‡
A_2	3.34 ± 0.05**‡	181.43 ± 1.80**‡	1.39 ± 0.03**‡	5.09 ± 0.25**‡
A_3	3.09 ± 0.06**‡	174.67 ± 6.20**‡	1.15 ± 0.04**†	4.49 ± 0.18**‡
B_1	3.29 ± 0.04**‡	159.65 ± 4.09**‡	1.41 ± 0.03**‡	4.93 ± 0.11**‡
B_2	2.98 ± 0.08**‡	145.68 ± 3.75**†	1.19 ± 0.02**‡	3.88 ± 0.26**†
B_3	2.76 ± 0.04**	131.11 ± 5.56**	1.04 ± 0.03**	2.99 ± 0.07**

[a] A_1, A_2, and A_3 are monomers with drug concentrations of 0.33, 0.495, and 0.66, respectively; B_1, B_2, and B_3 are micelles with drug concentrations of 0.33, 0.495, and 0.66, respectively, compared with the control group, $^{\#}P < 0.05$, $^{\#\#}P < 0.01$; 0.01; compared with model group, $^{*}P < 0.05$, $^{**}P < 0.01$; compared with B3, †$P < 0.05$, ‡$P < 0.01$.

4 Discussion

In the preliminary preparation methods, the film dispersion method, solvent volatilization method, and the choice of organic phase were investigated respectively.

This study investigated the physicochemical properties of BEL@HS15 prepared by the best preparation process. The particle size of nano micelles plays a crucial role in their transport *in vivo*. The appropriate particle size can avoid rapid glomerular filtration and increase biological distribution *in vivo*, without potential toxic effects in the body, which are due to unwanted accumulation of drugs and polymers.[8] Therefore, it can efficiently carry drugs to the lesion site. Nano particle size analyzer and transmission electron microscope were used for particle size detection and visual observation of nano micelles. The results show that nano micelles had small particle sizes and were evenly distributed in solution. In storage and system for dosing, nano micelle will be diluted in the body by lots of body fluids. When the concentration is lower than CMC, nano micelle is dissociated with wrapped drug sedimentation occurring, thereby leading to efficacy or side effects. Good dilution stability is a necessary condition for drugs to play their role, so storage stability and dilution stability become important indicators for the stability of nano-micelles.[18] The experimental results show that the micelle has good dilution stability. Pre-experiments confirmed that the size, PDI and z-potential of the prepared systems were not statistically different in the presence of albumin/FBS, and did not affect the stability of bellidifolin nano-micelles. Another feature of nano micelles is that they can release drugs slowly, avoid toxic and side effects caused by the sudden release of drugs, reduce drug dosage and improve drug efficacy at the same time.[19] Cumulative release rate detection is a simple and effective quality control method. The *in vitro* cumulative release rates of BEL@HS15 and BEL were compared by dialysis method to evaluate the quality and effectiveness of the preparation. It was shown that BEL@HS15 had the characteristic of slow drug release. The release curve was fitted and BEL@HS15 conformed to the primary release model, laying the theoretical foundation for further development and application of BEL@HS15.

Myocardial fibrosis (MF) is mediated by cardiac fibroblasts, which account for two-thirds of the total number of mammalian heart cells and are the most abundant cell in the heart.[20] It plays a key role in protecting myocardial extracellular matrix (ECM) homeostasis and wound healing after myocardial injury. Pathological damage to the heart can lead to a severe inflammatory response in the myocardial tissue, which leads to the accumulation of macrophages and neutrophils. Neutrophils secrete a variety of cytokines and growth factors, including TGF-β1, which binds to TGF-β1 receptor to activate the TGF-β/Smad pathway in cardiac fibroblast and upregulate transcription of ECM proteins and α-SMA. These ECM proteins are converted into myofibroblasts,[21] and the extracellular deposition of a large number of these ECM proteins will form fibrotic scar tissue, which is tough and inflexible, thus leading to pathological changes in the heart, such as myocardial infarction, heart failure, arrhythmia and other cardiovascular diseases.[22] TGF-β/Smad pathway is the most classic pathway to induce myocardial fibrosis, TGF-β1 and IITGF-β receptor (TβRII) binding, therefore TβRII is activated. Then recruit typeITGF-β receptor (TβRI) on the cell membrane to form a heterodimer, activated TβRII can make TβRI phosphorylation. Further, the activity of receptor serine protein kinase is activated, thus the expression of downstream regulatory factors Smad-2 and Smad-3 are increased and phosphorylated. The phosphorylated Smad-2 and Smad-3 combine with Smad-4 to form a complex and transfer to the nucleus to play a role in transcriptional regulation, which can mediate the increase of ECM protein and α-SMA synthesis in ECM.[23] And a large amount of ECM deposition promotes myocardial fibrosis, which in turn promotes the secretion of TGF-β1, causing a vicious cycle. The main pathological manifestations of MF are an excessive proliferation of myocardial fibroblasts, excessive deposition of ECM, and transformation to myofibroblasts.[24] Therefore, the CCK-8 method was used in this study to detect the abnormal proliferation of myocardial fibroblasts. ECM protein mainly includes myocardial Collagen fibroin, which is mainly composed of Collagen I and III. Collagen I is the main structural protein that constitutes the extracellular framework. Collagen I accounts for about 85% of the total amount of Collagen in the myocardium, responsible for establishing thick fibre and endowing them with tensile strength. Collagen III, which accounts for 11% of the total collagen protein of the normal heart, is aggregated in the form of microfibers and is responsible for the elasticity of the matrix network. The balance between ECM synthesis and degradation is crucial for maintaining the integrity of the heart structure.[1] α-SMA is a marker of myocardial fibroblasts activation.[25] The expression of more α-SMA and MF is closely related to TGF-β/Smad classic pathway. Smad-2 enters the cell nucleus to transcribe and regulate, leading to the transformation of cells, thus mediating the deposition of myocardial collagen fibrin. Collagen I, Collagen III, α-SMA and Smad-2 were selected as detection indexes in this study, and morphological observation method was used to observe the changes of cell morphology, to explore the pharmacodynamic effect of BEL on the treatment of myocardial fibrosis. The experimental results showed that the drug-loaded micelles with the same concentration had a higher inhibitory rate on the proliferation of fibroblasts than BEL, and the inhibition rate was concentration-dependent.

5 Conclusions

In this study, BEL was taken as the research object, HS15 was used as the carrier material, and it was prepared into BEL@HS15 by a solvent evaporation method, in order to improve the oral absorption and drug efficacy of BEL. The particle size, potential, microstructure, and stability of BEL@HS15 were investigated under the optimum preparation conditions. The sustained-release properties of BEL@HS15 were confirmed by *in vitro* release test. BEL cell uptake *in vitro* and anti-myocardial fibrosis efficacy tests were studied using myocardial fibroblasts as models. It was confirmed that BEL@HS15 could significantly inhibit myocardial fibrosis. In

this experiment, by selecting preparation methods and optimizing the preparation process, BEL nano micelles with appropriate particle size, high encapsulation rate, good stability, and slow-release effect were successfully prepared in this experiment. The preparation improved the problem of poor water-solubility of BEL, and effectively improved the anti-myocardial fibrosis effect. It provides a theoretical reference for further development and clinical application of BEL in the future.

Conflicts of interest

There are no conflicts to declare.

Acknowledgements

The Project was Supported by Open Research fund of State Key Laboratory of Drug Delivery and Pharmacokinetics, Tianjin Institute of Pharmaceutical Research, Tianjin 300301, People's Republic of China (No. 10162005) and the Fundamental Research Funds for Hebei University of Chinese Medicine, Shijiazhuang 050091, People's Republic of China (JYZ2020002).

References

1 L. Li, Q. Zhao and W. Kong, *Matrix Biol.*, 2018, **68–69**, 490–506.
2 D. N. Olennikov, N. K. Chirikova and C. Vennos, *Nat. Prod. Commun.*, 2017, **12**, 55–56.
3 Z. Wang, Q. Wu, Y. Yu, C. Yang, H. Jiang, Q. Wang, B. Yang and H. Kuang, *J. Ethnopharmacol.*, 2015, **174**, 261–269.
4 L. Li-Juan and L. Min-Hui, *Biochem. Syst. Ecol.*, 2009, **37**, 497–500.
5 A. Y. Li, J. J. Wang, S. C. Yang, Y. S. Zhao, J. R. Li, Y. Liu, J. H. Sun, L. P. An, P. Guan and E. S. Ji, *Biomed. Pharmacother.*, 2019, **110**, 733–741.
6 H. X. Yang, G. R. Xu, C. Zhang, J. H. Sun, Y. Zhang, J. N. Song, Y. F. Li, Y. Liu and A. Y. Li, *Int. J. Mol. Med.*, 2020, **45**, 223–233.
7 H. X. Yang, J. H. Sun, T. T. Yao, Y. Li, G. R. Xu, C. Zhang, X. C. Liu, W. W. Zhou, Q. H. Song, Y. Zhang and A. Y. Li, *Front. Pharmacol.*, 2021, **12**, 644886.
8 N. Majumder, N. G. Das and S. K. Das, *Ther. Delivery*, 2020, **11**, 613–635.
9 G. S. Kwon, *Crit. Rev. Ther. Drug Carrier Syst.*, 2003, **20**, 357–403.
10 I. Pepić, J. Lovrić and J. Filipović-Grčić, *Eur. J. Pharm. Sci.*, 2013, **50**, 42–55.
11 S. S. Kesharwani, S. Kaur, H. Tummala and A. T. Sangamwar, *Colloids Surf., B*, 2019, **173**, 581–590.
12 L. Illum, F. Jordan and A. L. Lewis, *J. Controlled Release*, 2012, **162**, 194–200.
13 A. Leonardi, C. Bucolo, G. L. Romano, C. B. Platania, F. Drago, G. Puglisi and R. Pignatello, *Int. J. Pharm.*, 2014, **470**, 133–140.
14 J. Hou, E. Sun, C. Sun, J. Wang, L. Yang, X. B. Jia and Z. H. Zhang, *Int. J. Pharm.*, 2016, **512**, 186–193.
15 L. Liu, K. Mao, W. Wang, H. Pan, F. Wang, M. Yang and H. Liu, *AAPS PharmSciTech*, 2016, **17**, 757–766.
16 X. Huang, W. Liao, G. Zhang, S. Kang and C. Y. Zhang, *Int. J. Nanomed.*, 2017, **12**, 2215–2226.
17 J. Aguiar, P. Carpena, J. A. Molina-Bolívar and C. Carnero Ruiz, *J. Colloid Interface Sci.*, 2003, **258**, 116–122.
18 A. K. Jannu, E. R. Puppala, B. Gawali, N. P. Syamprasad, A. Alexander, S. Marepally, N. Chella, J. K. Gangasani and V. G. M. Naidu, *Int. J. Pharm.*, 2021, **605**, 120819.
19 X. Gao, F. Zheng, G. Guo, X. Liu, R. Fan, Z. Y. Qian, N. Huang and Y. Q. Wei, *J. Mater. Chem. B*, 2013, **1**, 5778–5790.
20 A. Deb and E. Ubil, *J. Mol. Cell. Cardiol.*, 2014, **70**, 47–55.
21 S. Bolivar, J. A. Espitia-Corredor, F. Olivares-Silva, P. Valenzuela, C. Humeres, R. Anfossi, E. Castro, R. Vivar, A. Salas-Hernández, V. Pardo-Jiménez and G. Díaz-Araya, *Cytokine*, 2021, **138**, 155359.
22 S. Redondo, J. Navarro-Dorado, M. Ramajo, Ú. Medina and T. Tejerina, *Vasc. Health Risk Manage.*, 2012, **8**, 533–539.
23 J. C. Liu, F. Wang, M. L. Xie, Z. Q. Cheng, Q. Qin, L. Chen and R. Chen, *Int. J. Cardiol.*, 2017, **228**, 388–393.
24 X. L. Zhou, Y. H. Fang, L. Wan, Q. R. Xu, H. Huang, R. R. Zhu, Q. C. Wu and J. C. Liu, *J. Cell. Physiol.*, 2019, **234**, 8834–8845.
25 C. Fix, A. Carver-Molina, M. Chakrabarti, M. Azhar and W. Carver, *J. Cell. Physiol.*, 2019, **234**, 13931–13941.